Med Biol Eng Comput (2014) 52:343–351
DOI 10.1007/s11517-013-1135-5

ORIGINAL ARTICLE

Frequency range extension of spectral analysis of pulse rate variability based on Hilbert–Huang transform

Chia-Chi Chang · Tzu-Chien Hsiao · Hung-Yi Hsu

Received: 26 February 2013 / Accepted: 21 December 2013 / Published online: 17 January 2014

Abstract Heart rate variability (HRV) is a well-accepted indicator for neural regulatory mechanisms in cardiovascular circulation. Its spectrum analysis provides the powerful means of observing the modulation between sympathetic and parasympathetic nervous system. The timescale of HRV is limited by discrete beat-to-beat time intervals; therefore, the exploration region of frequency band of HRV spectrum is relatively narrow. It had been proved that pulse rate variability (PRV) is a surrogate measurement of HRV in most of the circumstances. Moreover, arterial pulse wave contains small oscillations resulting from complex regulation of cardiac pumping function and vascular tone at higher frequency range. This study proposed a novel instantaneous PRV (iPRV) measurement based on Hilbert–Huang transform. Fifteen healthy subjects participated in this study and received continuous blood pressure wave recording in supine and passive head-up tilt. The result showed that the very-high-frequency band (0.4–0.9 Hz) varied during head-up tilt and had strong correlation ($r = 0.77$) with high-frequency band and medium correlation ($r = 0.643$) with baroreflex sensitivity. The very-high-frequency band of iPRV helps for the exploration of non-stationary autoregulation and provides the non-stationary spectral evaluation of HRV without distortion or information loss.

Keywords Heart rate variability · Pulse rate variability · Hilbert–Huang transform

Abbreviations

HR	Heart rate
RRi	Beat-to-beat interval
ECG	Electrocardiogram
HRV	HR variability
ANS	Autonomic nervous system
SNS	Sympathetic nervous system
PNS	Parasympathetic nervous system
FFT	Fast Fourier transform
LF	Low frequency
HF	High frequency
PRV	Pulse rate variability
HHT	Hilbert–Huang transform
EMD	Empirical mode decomposition
IMFs	Intrinsic mode functions
EEMD	Ensemble EMD
CEEMD	Complementary EEMD
ABP	Arterial blood pressure
IF	Instantaneous frequency
HT	Hilbert transform
NHT	Normalized HT
iPRV	Instantaneous PRV
$EtCO_2$	End-tidal CO_2
HUT	Head-up tilt

C.-C. Chang
Institute of Computer Science and Engineering, National Chiao Tung University, Hsinchu, Taiwan, ROC

T.-C. Hsiao
Department of Computer Science, Institute of Biomedical Engineering; Biomedical Electronics Translational Research Center and Biomimetic Systems Research Center, National Chiao Tung University, Hsinchu, Taiwan, ROC

H.-Y. Hsu
Department of Neurology, Chung Shan Medical University, Taichung, Taiwan, ROC

H.-Y. Hsu (✉)
Section of Neurology, Department of Internal Medicine, Tungs' Taichung Metro Harbor Hospital, No. 699, Sec. 1, Jhongci Road, Wuci District, Taichung 435, Taiwan, ROC
e-mail: hungyihsu@gmail.com

FM	Frequency modulation
iPR	Instantaneous PR
LH ratio	Low–high ratio

1 Introduction

Heart rate (HR) is regulated by autonomic nervous system (ANS) and varies over time in healthy subjects. Previous studies showed that the variability of HR (HRV) could be measured by beat-to-beat intervals (RRi) between consecutive R waves on electrocardiogram (ECG) [19, 21]. The ANS contains sympathetic nervous system (SNS) and parasympathetic nervous system (PNS). The modulation of PNS and SNS is important for cardiovascular circulation and can be monitored by the spectral analysis of HRV [1, 14]. Most studies adopted fast Fourier transform (FFT) for the frequency-domain analysis of HRV. Several studies showed that the short-term HRV spectrum contained two major frequency bands, which are used as the indicators of ANS activation. The low-frequency (LF) range (0.04–0.15 Hz) presents the SNS activities, while the high-frequency (HF) range (0.15–0.4 Hz) is mainly regulated by the PNS activities [19, 21]. Though the effect of physiological controls in these frequency bands has been demonstrated, the feasibility and the reproducibility are still restricted in HRV studies [10]. An alternative measurement of HRV, called pulse rate variability (PRV), was proposed. PRV replaces ECG recording in HRV with photoplethysmography and is capable to assess the ANS activities during non-stationary conditions [9]. Moreover, Gil's study examined that PRV is as a surrogate of HRV during non-stationary conditions, in particular, during the tilt table test. The arterial pulse wave contains small oscillations resulting from complex regulation of cardiac pumping function, respiratory movement, and vascular tone. Therefore, PRV provides not only ANS activities but also the information of peripheral circulation.

Conventional frequency-domain analysis of HRV has several limitations. The time resolution of HRV was limited by tachogram, which adopted the interpolation method in spectral analysis [5]. Besides, FFT and discrete wavelet transform are based on linear stationary mathematic model and cannot represent the non-stationary characteristics. Recently, a novel adaptive method, called Hilbert–Huang transform (HHT) [11], had been proposed by Huang and has been used widely in data-processing research in many fields. It has the capability dealing with non-stationary and nonlinear data owing to its essential preprocess called empirical mode decomposition (EMD). EMD extracts the finite set of components, named intrinsic mode functions (IMFs), from source non-stationary data. The IMFs adaptively represent the features of source data without distortion and had been adopted for HRV analysis [7, 18, 28].

Empirical mode decomposition served as an adaptive dyadic filter bank [8]. However, EMD contains the intermittency phenomenon, called mode-mixing problem, owing to the sensitivity of interpolation methods, stop criterion of IMF, and the end effect [11]. The mode-mixing problem was eliminated by noise-assisted data analysis method, known as ensemble EMD (EEMD) [25]. The ensemble IMFs are computed by averaging each corresponding IMF decomposed from different mixtures of added noise and source data. But EEMD is still insufficient for non-stationary intrinsic characterization owing to its nonzero noise residue. The noise residue was reduced by adding positive and negative white noises, respectively, as two mixtures of the added noise and source data, which called complementary EEMD (CEEMD) [29]. CEEMD extends the concept of EEMD and eliminates the residue of added noise in IMFs. Several studies applied these kinds of EMD for medical data process [4, 17, 23, 24]. But the resolution of multiple timescales is still a major limitation of HRV spectral analysis.

The continuous-time component related to heartbeat can be extracted from arterial blood pressure (ABP) signal as a simple fluctuation signal with heartbeat rhythm by EMD [12, 26]. The continuous-time heartbeat rhythm, known as HR in uniform timescale, can be obtained by calculating the instantaneous frequency (IF) of heartbeat component [26]. Though the IF can be calculated by Hilbert transform (HT) [11], the estimated IF might be wrong with negative value. According to Bedrosian's theorem, the orthogonal complex pair of simple oscillation was calculated by HT only if there is no amplitude modulation in source data. The amplitude modulation was eliminated by normalization method of normalized HT (NHT) [12]. Furthermore, according to Nuttall's theorem, the complex pair of source data was calculated by HT only if the oscillation of source data is sinusoidal-like signal, which means the source data only contains simple oscillation. Because the heartbeat-related component only contains the HR rhythm, it is simple enough to get the correct result from HT [12].

The aim of this study was (1) to estimate the HRV by instantaneous pulse rate variability (iPRV) by HHT; (2) to explore new frequency band with much precise time resolution in frequency domain.

2 Methods

2.1 Subjects and data collection

All measurements were performed in a quiet temperature-controlled room. The beat-to-beat ABP was recorded by Task Force® Monitor equipped with a servo-controlled plethysmography (CNSystems, Medizintechnik AG, Graz,

Austria). ECG, thoracic impedance, and end-tidal CO_2 ($EtCO_2$; RespSenseTM $EtCO_2$, Nonin Medical Inc.) concentration were recorded simultaneously with 200 Hz sampling rate. The baroreflex sensitivity was calculated by the sequence method [13, 15] and was exported from Task Force® Monitor.

Fifteen healthy subjects (9 males; age 43 ± 17), who did not have the history of cardiovascular disease, participated in this study. All recruited subjects were asked to rest quietly in supine position for 10 min. After all recorded signals were stabilized, a 10-min baseline recording was performed under spontaneous breathing. Then, participants were tilting up passively on the automatic tilting table and kept in the tilt-up position for 10 min as head-up tilt (HUT) experiment. This study was approved by institutional review board of this hospital. Informed consent was obtained from all subjects before the experiment.

2.2 Ensemble empirical mode decomposition

The IMFs are computed by sifting process, as an iteratively detrending operation. The essence of sifting process is based on energy-associated extraction with each timescale. The timescale is determined by the locations of local extrema. The sifting process of EMD contains several steps. First, the local extrema of the time series $x(t)$ are identified by peak-valley detection. The upper envelope $U(t)$ and lower envelope $L(t)$ are generated by cubic spline interpolation according to the local maxima and the local minima, respectively. Both $U(t)$ and $L(t)$ cover $x(t)$ in current timescale. The trend in current timescale is computed by calculating the mean of $U(t)$ and $L(t)$.

$$m(t) = (U(t) + L(t))/2 \tag{1}$$

The sifting process subtracted the trend from original time series $x(t)$, as detrending operation.

$$h_1(t) = x(t) - m_1(t) \tag{2}$$

And the subtraction was iteratively performed

$$\begin{cases} h_{11}(t) = x(t) \\ h_{1k}(t) = h_{1(k-1)}(t) - m_{1k}(t), \quad k > 1 \end{cases} \tag{3}$$

k presented the number of detrending operation. $h_{1k}(t)$ was considered as an IMF only if the trend $m_{1k}(t)$ satisfies the criterion as the steady constant trend.

$$h_{1k}(t) = \mathrm{IMF}_1(t) \tag{4}$$

The first residue was computed.

$$r_1(t) = x(t) - \mathrm{IMF}_1(t) \tag{5}$$

The residue $r_i(t)$ was the target of ith iteration of EMD for $\mathrm{IMF}_i(t)$ computation, and $x(t)$ performed at the first iteration for $\mathrm{IMF}_1(t)$. After n iteration, $x(t)$ was decomposed into n IMFs, $\mathrm{IMF}_1(t) \sim \mathrm{IMF}_n(t)$, and one residue, $r_n(t)$, which was either the steady trend or a constant.

$$x(t) = \sum_{i=1}^{n} \mathrm{IMF}_i(t) + r_n(t) \tag{6}$$

EMD decomposes the non-stationary data into finite set of IMFs without information loss or distortion. The mode-mixing problem, which means that one IMF contains multiple characteristics rather than monotonic characteristics as monocomponent, was eliminated by a noise-assisted EMD, called EEMD. For elimination of noise residue in EEMD, CEEMD was proposed and produced much stabilized and consistent results of IMFs. This study used CEEMD for the ABP signals decomposition as feature extraction method.

2.3 Determination of IMF

IMF, as the monocomponent, contains monotonic characteristic and its trend approximates zero at any time instant [27]. However, the mean envelope, as the trend, is hard to achieve zero owing to the interference of non-stationary signal. Stop criterion, a recognized method for steady trend determination, is an important issue of EMD and determines the feasibility of the decomposition results. The mean value criterion [20] was adopted in this study, which was able to produce the consistent IMF in non-stationary conditions [6].

2.4 Instantaneous frequency by normalized Hilbert transform

The instantaneous frequency presents how frequent the oscillation of source data is at specific time instant, which can be computed by NHT. NHT contains several steps. First, the amplitude modulation of source data $x(t)$ was eliminated by iteratively normalization [12]. Then, the Hilbert pair, $y(t)$, of frequency modulation (FM) part of source data, $x_{\mathrm{FM}}(t)$, was calculated by HT, $H(x_{\mathrm{FM}}(t))$, and represented the complex pair in complex plane.

$$y(t) = H(x_{\mathrm{FM}}(t)) = \frac{1}{\pi} P.V. \int_{-\infty}^{\infty} \frac{x_{\mathrm{FM}}(\tau)}{t - \tau} \mathrm{d}\tau \tag{7}$$

$$A(t)e^{j\omega(t)} = x_{\mathrm{FM}}(t) + jy(t) \tag{8}$$

The instantaneous frequency was obtained by the differential of the instantaneous phase $\omega(t)$, which was calculated from the complex composition of $x_{\mathrm{FM}}(t)$ and its complex pair $y(t)$.

$$\omega(t) = \tan^{-1} \frac{y(t)}{x_{\mathrm{FM}}(t)} \tag{9}$$

$$\omega'(t) = \frac{x_{FM}(t)y'(t) - y(t)x'_{FM}(t)}{x_{FM}(t)^2 + y(t)^2} \quad (10)$$

According to Bedrosian's theorem, the orthogonality between $x_{FM}(t)$ and $y(t)$ was verified by polar plot in complex plane.

2.5 Instantaneous pulse rate variability

The steps of iPRV were shown in Fig. 1. The IMF_4 of ABP extracted by CEEMD was used as the continuous-time heartbeat-related component [6] in this study, and its oscillations were consistent with HR rhythm at each time instant (Fig. 2). The instantaneous frequency of heartbeat-related component was computed by NHT. The instantaneous pulse rate (iPR) was estimated by the inversion of instantaneous frequency of IMF_4 in order to compare with the RRi series. The wavelet analysis was applied for the detrend process as the trend (<0.01 Hz) elimination (Fig. 1b). The amplitude modulation of heartbeat-related component was eliminated obviously individually (Fig. 3). The FM of IMF_4 of ABP waveform (Fig. 3) presented a simple sinusoidal-like fluctuation. The orthogonality was good that its polar plot presented a clear unit circle for all of the heartbeats during 10-min recording. The FFT was applied for power spectral estimation in each frequency band, including LF, HF, and VHF. The spectral analysis programs used in this study was developed by using commercial software (LabVIEW version 2011, National Instruments Corp., Austin, USA).

2.6 Statistic analysis

Paired-sample t test was used to compare the significant difference between the percentage changes of spectral power in each frequency band during supine and HUT. The percentage change was calculated by dividing the spectral power by total power. P value of <0.05 was considered significant. Pearson's correlation coefficient was calculated with different indices, and P value <0.01 was considered as significant correlation. All statistical analysis was performed by using commercial statistics software (Statistical Package for Social Science, version 15.0, SPSS Inc., Chicago, Illinois).

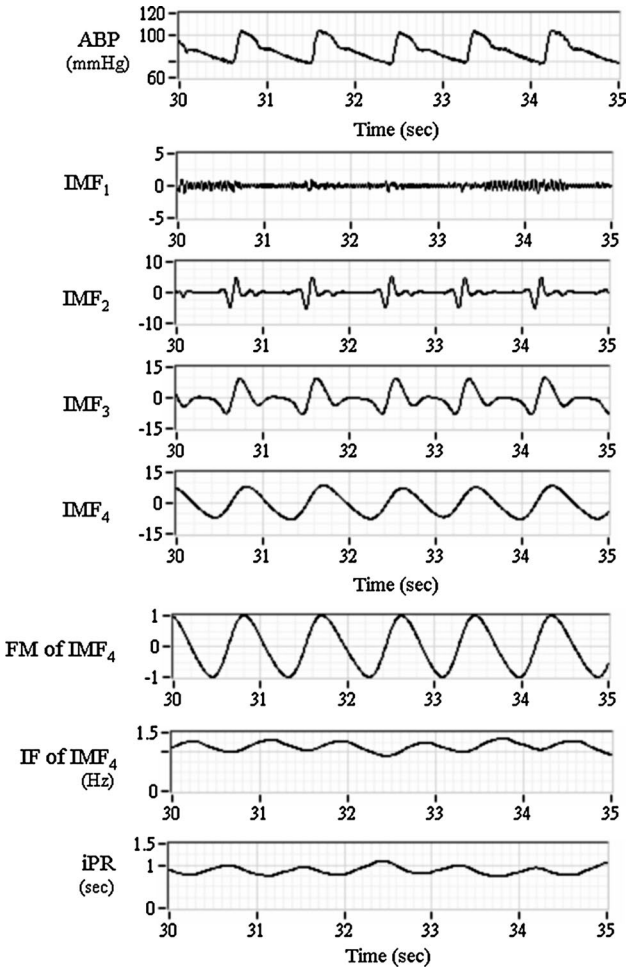

Fig. 2 Results of CEEMD and NHT for ABP waveform. *Top graph* presents the original ABP waveform, IMF_1–IMF_4, the FM of IMF_4, and instantaneous frequency (IF) of IMF_4 are listed below, and the bottom graph is iPR estimated by the inversion of IF of IMF_4

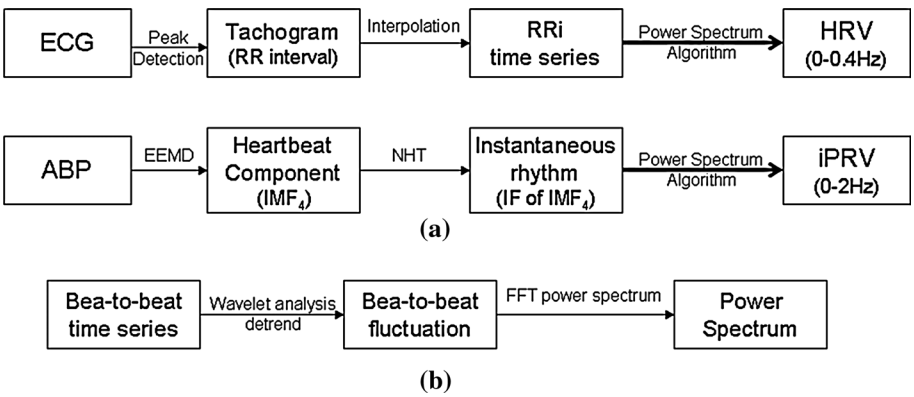

Fig. 1 **a** Flow chart of instantaneous pulse rate variability (iPRV) compared with heart rate variability (HRV). **b** Power spectrum algorithm

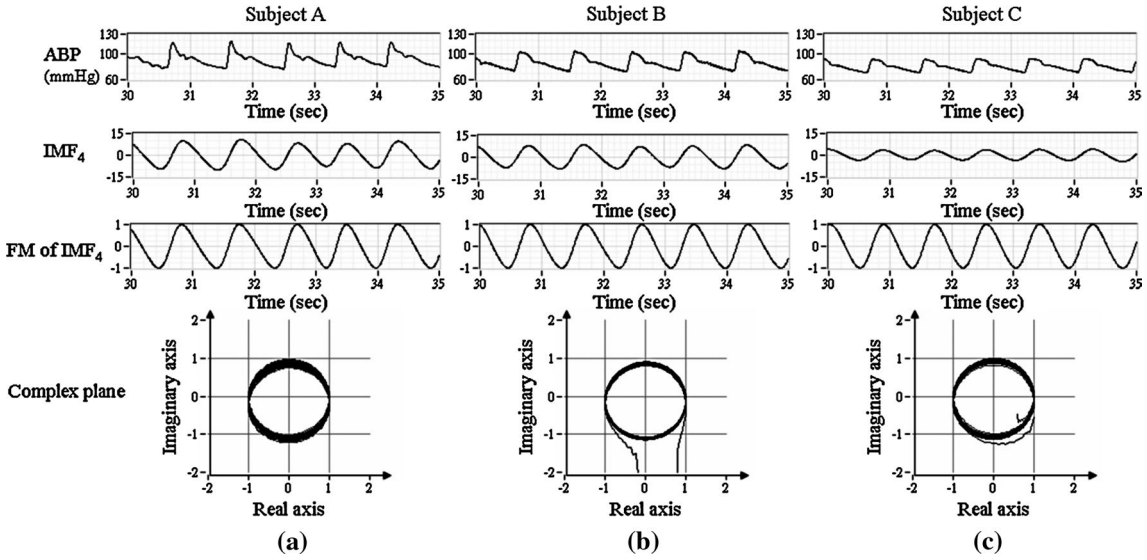

Fig. 3 Results of the orthogonality for three different kinds of ABP waveform in three different subjects. All panels represent orthogonality of NHT. From the top graph to the bottom graph showed the original ABP waveform, the corresponding IMF_4, the FM of each IMF_4, and the polar plot of FM of IMF_4, and its Hilbert pair for orthogonality verification

3 Results

3.1 Instantaneous pulse rate variability (iPRV)

The RRi series and iPR series were observed in Fig. 4a. The iPR series had synchronous changes with RRi series and contained much more fluctuations with higher time resolution as intra-wave frequency modulation of heartbeat-related component [12]. Conventional HRV spectrum contained two major frequency bands in short-term ANS evaluation, including LF (0.04–0.15 Hz) and HF (0.15–0.4 Hz) (Fig. 4b). The amplitude of iPR series and the power of iPR spectrum decreased during HUT [9, 21]. Furthermore, the power of iPRV in very-high-frequency band (VHF, 0.4–0.9 Hz) decreased during HUT. The HR was observed in iPRV spectrum with the highest power magnitude in the frequency band around 1 Hz (0.9–1.5 Hz) as the main carrier of iPR. The iPRV spectrum indicated that the HR increased during HUT.

The spectral analysis of HRV and iPRV was summarized in Table 1. In HRV spectrum, the power of LF decreased and the percentage of LF increased during HUT [9, 21]. The changes in LF, including its power and its percentage, were not statistically significant. Both the power of VHF and the percentage of VHF were small in HRV spectrum. The correlations of the power between HRV spectrum and PRV spectrum are 0.999, 0.989, 0.763 in LF, HF, VHF, respectively, in baseline and are 0.999, 0.985, 0.514 in LF, HF, VHF, respectively, during HUT. The correlations of the power between HRV spectrum and iPRV spectrum are 0.965, 0.949, 0.864 in LF, HF, VHF, respectively, in baseline and are 0.82, 0.953, 0.809 in LF, HF, VHF, respectively, during HUT. The power of HF and the percentage of HF decreased significantly during HUT. In iPRV spectrum, the power of LF decreased non-significantly, and the percentage of LF was not significantly different during HUT. The power of HF and the percentage of HF decreased after HUT. The power of VHF decreased and the percentage of VHF increased significantly in HUT test. Furthermore, the power of VHF was significantly correlated with the power of HF ($r = 0.77$) and with the power of LF ($r = 0.5$). The power of VHF had significant relationship ($r = 0.643$) with baroreflex sensitivity, while the percentage of VHF had significant negative correlation ($r = -0.59$) with baroreflex sensitivity. The relevant scatter plots were illustrated in Fig. 5.

4 Discussion

It had been examined that the PRV is a surrogate of HRV analysis during non-stationary conditions, in particular, during HUT [9]. The results in this study showed the consistent investigation with high correlation between PRV spectrum and HRV spectrum. Moreover, this study showed that the results of iPRV were highly consistent with those of conventional HRV in LF and HF bands. In addition, the novel spectral analysis of iPRV improved the time resolution of PR series by iPR series based on HHT, therefore, it was able to explore the new frequency band, called VHF. The VHF was related to baroreflex and HF power and could be a potential indicator of PNS activities. The analysis of iPRV has potential for quantitative evaluation of the

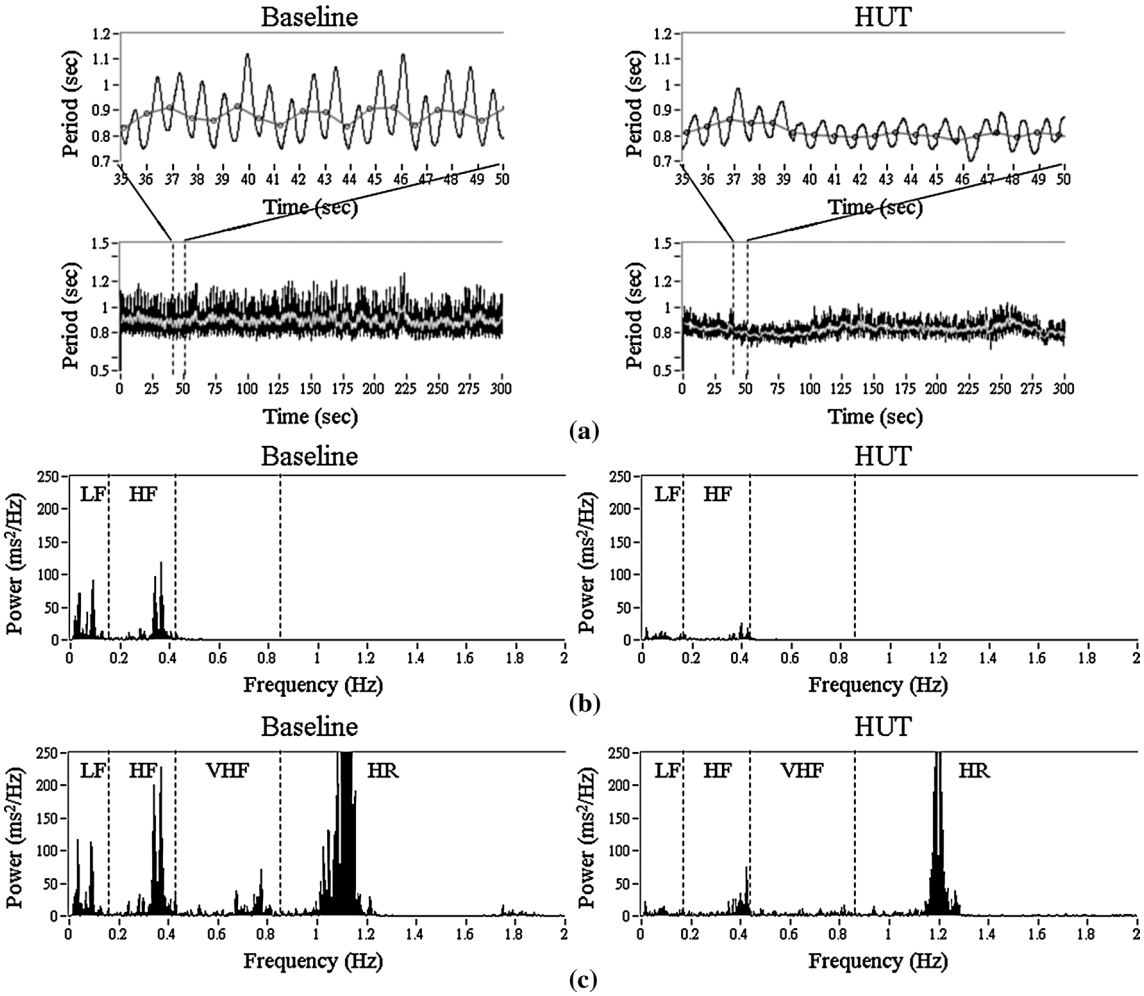

Fig. 4 Illustration of power spectrum of iPRV and HRV during baseline (*left panel*) and HUT (*right panel*). **a** RRi series (*gray dotted line*) and iPR series (*black line*) of 15-s (*upper*) and 5-min (*lower*) periods; **b** the power spectrum of HRV, **c** the power spectrum of iPRV

Table 1 Spectral analysis of conventional short-term heart rate variability (HRV) and instantaneous pulse rate variability (iPRV)

	Baseline		Head-up tilt	
	HRV	iPRV	HRV	iPRV
LF (ms^2)	669.5 ± 908.9	888.83 ± 1205.89	316.5 ± 308.6	344.0 ± 296.9
HF (ms^2)	1062.9 ± 1192.4	1905.0 ± 1904.9	348.0 ± 426.5[§]	623.3 ± 626.0[§]
VHF (ms^2)	59.3 ± 110.9	1359.8 ± 1524.2	34.4 ± 47.9	725.8 ± 697.7
LF/TP (%)	27.2 ± 8.5	20.8 ± 8.3	32.7 ± 15.6	19.9 ± 8.3
HF/TP (%)	42.7 ± 17.2	43.6 ± 11.7	28.7 ± 17.6[§]	34.3 ± 15.8*
VHF/TP (%)	6.2 ± 9.1	35.6 ± 10.6	8.4 ± 8.6	45.8 ± 17.0*

LF low-frequency band (0.04–0.15 Hz), *HF* high-frequency band (0.15–0.4 Hz),*VHF* very-high-frequency band (0.4–0.9 Hz),*TP* total power within the whole frequency band (0–0.9 Hz)

* $P < 0.05$ compared with baseline

§ $P < 0.01$ compared with baseline

physiological control in new frequency band and helps to discover the non-rhythmic mechanism of autoregulation in cardiovascular circulation.

Previous study demonstrated that EMD could act as a filter bank adaptively [8] without composited phase distortion, which existed in conventional band-pass filter.

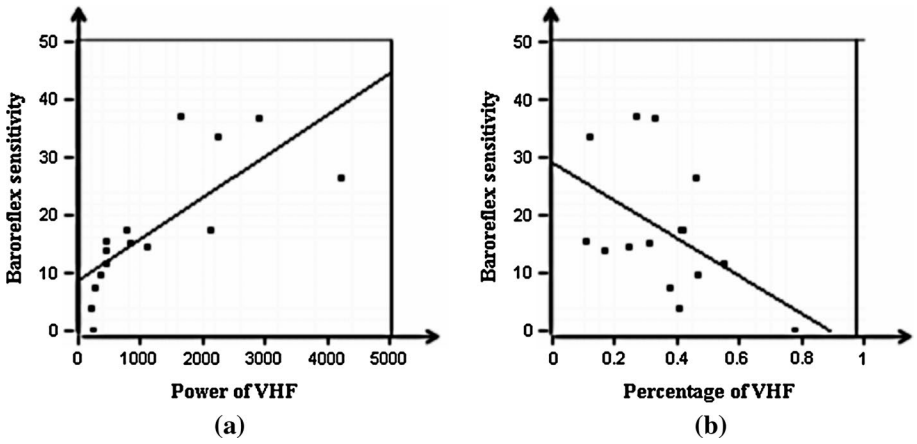

Fig. 5 Scatter plot of **a** the power of VHF and baroreflex sensitivity; **b** the percentage of VHF and baroreflex sensitivity with total fifteen healthy subjects

Our results showed that the component related to heartbeat (IMF_4) could be extracted well form ABP signal by CEEMD. The heartbeat rhythm was presented by heartbeat-related component as the simple sinusoidal fluctuation. By the normalization method, the amplitude modulation was eliminated from heartbeat component and the FM of the component related to heartbeat had good orthogonality individually (Fig. 3). The amplitude modulation of heartbeat-related component varied along with pulse pressure, therefore, it could potentially be used for pulse pressure related study, such as pulse pressure variation [22]. The iPR was computed by NHT and presented the continuous-time PR, as the intra-wave frequency modulation of the component related to heartbeat. It had been proved that the intra-wave frequency modulation presented much more physical meaning in nature [12]. By analysis of intra-wave frequency modulation of the component related to heartbeat, the frequency band of HRV could extend the exploration region widely owing to increasing time resolution. The time resolution increased from discrete-time tachogram into continuous-time measurement (Fig. 4a). Moreover, iPR series fluctuated in much higher time resolution than RRi series, and RRi series might be one of the fluctuation trends of iPR series.

Traditionally, there are mainly three frequency bands of non-rhythmic neural regulatory in cardiovascular circulation in short-term ECG recording. Most studies examined that LF presented the SNS activities and HF presented the PNS activities. VHF is much less defined in short-term recording [9, 21]. Most of HF is coupling respiration frequency (0.1–0.3 Hz) and presented the interaction between PNS, respiration, and cardiorespiratory coupling. The changes in these frequency bands were quantitatively measured by spectral power, normalized unit power, and percentage change divided by total power. The modulation of SNS and PNS was evaluated by the ratio of LF and HF, called low–high ratio (LH ratio) [9, 21]. But LH ratio might underestimate the balance between SNS and PNS, and recent study examined that the percentage change provided much reliable evaluation [16].

The HRV analysis interpolated the discrete RRi into time series and converted the discrete multiple timescale into uniform timescale. The time resolution is limited by the beat-to-beat timescale of RRi in spite of high sampling rate in ECG recording. Therefore, the conventional HRV analysis cannot produce reliable result at higher-frequency band. The time axis of PR was continuous in uniform scale based on HHT, which called iPR. The iPRV spectrum demonstrated similar variation along with HRV spectrum in LF and HF during HUT. The decreasing power of HF indicated the decreasing PNS activities with increasing SNS activities for the compensation of temporary postural hypotension during HUT. Furthermore, the VHF (0.4–0.9 Hz) became more evident by the spectral analysis of iPRV. The power of VHF decreased significantly during HUT, and it was significantly correlated with the power of HF ($r > 0.7$). The percentage of VHF increased while the percentage of HF decreased. It might indicate the different dominant autoregulation mechanism during HUT. The main frequency peak of VHF was varied with different HR individually. Though VHF had significant correlation with baroreflex sensitivity, the linearity of the correlation was not strong (<0.7). VHF might contain the regulation frequency of baroreflex owing to the medium correlation. The results that the power of VHF decreased during HUT suggested that the VHF might be influenced by the activities of ANS at higher-frequency range, cardiac pumping function, the influence of cardiac performance related to respiration [2], and other cardiovascular autoregulation mechanism, such as baroreflex or peripheral vascular tone in non-stationary conditions. VHF was evaluated from iPRV and represented the non-stationary physical meaning of intra-wave frequency modulation of heartbeat rhythm based on HHT. However, pulse waveform was affected by peripheral regulation, such as arterial elasticity and peripheral resistance. These regulations might present by fluctuation of compound at specific frequency band in iPRV spectrum, which

needs further investigation and verification. In the higher-frequency band (0.9–2 Hz) of iPRV spectrum (Fig. 4c), the pulse rate was observed with the highest power magnitude. The higher PR indicated the compensatory increase in HR during HUT. Besides, Mateo et al. investigated that the power of VHF in HRV was obtained as the index for coronary artery disease diagnosis during exercise, while the mean HR was above 120 bpm [3]. The potential usefulness of the power of VHF in iPRV in the cardiovascular disease diagnosis also needs further investigation.

Although clinical evidences showed that ECG could be more relevant and physiologically meaningful for the study of rapid neural activities related to the cardiovascular regulation, iPRV measurement cannot be applied to ECG signal. iPRV is fundamentally based on EMD and NHT. Since ECG signal is the summation of multiple action potentials at each part of heart, it is difficult to extract the sinusoid-like wave function from ECG by EMD. If the extracted components are not sinusoid-like wave function, the results of NHT would be wrong according to Nuttall's theorem [12]. On the other hand, the blood pulse signal, such as ABP signal, is the synthesis of the stroke volume pulse and reflected wave, which are sinusoid-like function, and the waveform of blood pulse signal matches the requirement of iPRV measurement. In order to ensure that VHF band was not derived from the artifacts of ABP measurement by finger cuff, this study applied the iPRV measurement to ABP signal recorded by radial artery tonometer (Colin CBM-7000, Colin Medical Technology Corp., Mediana Technologies Corp., San Antonio, Texas, USA) at the wrist. The result showed substantial VHF band which was consistent with that obtained by finger photoplethysmography. Therefore, the variability found in VHF is associated with the physiological source rather than the device of ABP measurement.

Though iPRV analysis provided more information than traditional HRV analysis, it has some limitations. First, the precise iPR is on the premise of that every blood pulse generated successfully by each cardiac muscle contraction, which might fail in some specific circumstances, such as premature ventricular contractions. Second, the precision of iPR measurement depends on ABP measurements, such as pulse plethysmography. Blood pulse measurements are quite sensitive to patient and probe-tissue movement artifacts and the sensing equipment is more elaborate compared to ECG. Though EMD, as the filter bank, has the capability to deal with high-frequency noise caused by movement artifact, the automatic artifact detection and the replacement of corresponding corrupted signal segments are essential if the artifact breaks the morphology of the heartbeat fluctuation. Third, iPRV analysis depends on HHT. The selection of parameters setting of HHT and the property of source signal would influence the results. The time complexity of HHT belongs to non-deterministic polynomial time, and it is insufficient for real-time processing currently.

5 Conclusion

This study showed that the continuous-time HR rhythm could be evaluated by iPR based on HHT. The iPRV spectral analysis showed the consistent results with conventional HRV analysis that the correlation was good in each frequency band. In addition, the iPRV spectral analysis is able to examine the new frequency band-VHF-owing to the breakthrough of the limitation of time resolution. VHF is correlated with baroreflex sensitivity and PNS activities. The physiologic meanings of VHF need further investigation with large population for verification. The iPRV analysis provides a new approach to explore ANS function and helps for the quantitative evaluation on the non-rhythmic mechanism of cardiovascular autoregulation.

Acknowledgments Research supported by Taiwan National Science Council under Grant Number: NSC 100-2314-B-040-003, NSC-102-2220-E-009-001, NSC-102-2220-E-009-023 and NSC-102-2627-E-010-001 and in part by "Aim for the Top University Plan" of the National Chiao Tung University and Ministry of Education, Taiwan, R.O.C. This work was also supported in part by the UST-UCSD International Center of Excellence in Advanced Bioengineering sponsored by the Taiwan National Science Council I-RiCE Program under Grant Number: NSC-101-2911-I-009-101.

References

1. Akselrod S, Gordon D, Ubel FA, Shannon DC, Berger AC, Cohen RJ (1981) Power spectrum analysis of heart rate fluctuation: a quantitative probe of beat-to-beat cardiovascular control. Science 213:220–222
2. Babaeizadeh S, Zhou SH, Liu X, Hu WY, Feild DQ, Helfenbein ED, Gregg RE, Lindauer JM (2007) A novel heart rate variability index for evaluation of left ventricular function using five-minute electrocardiogram. Comput Cardiol 34:473–476
3. Bailón R, Mateo J, Olmos S, Serrano P, García J, del Río A, Ferreira IJ, Laguna P (2003) Coronary artery disease diagnosis based on exercise electrocardiogram indexes from repolarisation, depolarisation and heart rate variability. Med Biol Eng Comput 41:561–571
4. Balocchi R, Menicucci D, Santarcangelo E, Sebastiani L, Gemignani A, Ghelarducci B, Varanini M (2004) Derive the respiratory sinus arrhythmia from the heartbeat time series using empirical mode decomposition. Chaos Solitons Fractals 20:171–177
5. Berntson GG, Bigger Jr JT, Eckberg DL, Grossman P, Kaufmann PG, Malik M, Nagaraja HN, Porges SW, Saul JP, Stone PH, van der Molen MW (1997) Heart rate variability: origins, methods, and interpretive caveats. Psychophysiology 34:623–648
6. Chang CC, Hsu HY, Hsiao TC (2013) Quantitative non-stationary assessment of cerebral hemodynamics by empirical mode decomposition of cerebral Doppler flow velocity. Adv Adapt Data Anal 5:1350002. doi:10.1142/S1793536913500027
7. de Souza Neto EP, Abry P, Loiseau P, Cejka JC, Custaud MA, Frutoso J, Gharib C, Flandrin P (2007) Empirical mode

decomposition to assess cardiovascular autonomic control in rats. Fundam Clin Pharmacol 21:481–496
8. Flandrin P, Rilling G, Goncalves P (2004) Empirical mode decomposition as a filter bank. IEEE Signal Process Lett 11:112–114
9. Gil E, Orini M, Bailon R, Vergara JM, Mainardi L, Laguna P (2010) Photoplethysmography pulse rate variability as a surrogate measurement of heart rate variability during non-stationary conditions. Physiol Meas 31:1271–1290
10. Højgaard MV, Holstein-Rathlou NH, Agner E, Kanters JK (2005) Reproducibility of heart rate variability, blood pressure variability and baroreceptor sensitivity during rest and head-up tilt. Blood Press Monit 10:19–24
11. Huang NE, Shen Z, Long SR, Wu MC, Shih HH, Zheng Q, Yen NC, Tung CC, Liu HH (1998) The empirical mode decomposition and the Hilbert spectrum for nonlinear and nonstationary time series analysis. Proc R Soc Lond A 454:903–995
12. Huang NE, Wu Z, Long SR, Arnold KC, Chen X, Blank K (2009) On instantaneous frequency. Adv Adapt Data Anal 1:177–229
13. Hughson RL, Quintin L, Annat G, Yamamoto Y, Gharib C (1993) Spontaneous baroreflex by sequence and power spectral methods in humans. Clin Physiol 13:663–676
14. Kamath MV, Fallen EL (1993) Power spectral analysis of heart rate variability: a noninvasive signature of cardiac autonomic function. Crit Rev Biomed Eng 21:245–311
15. La Rovere MT, Pinna GD, Raczak G (2008) Baroreflex sensitivity: measurement and clinical implications. Ann Noninvasive Electrocardiol 13:191–207
16. Li H, Kwong S, Yang L, Huang D, Xiao D (2011) Hilbert–Huang transform for analysis of heart rate variability in cardiac health. IEEE/ACM Trans Comput Biol Bioinform 8:1557–1567
17. Lo MT, Hu K, Liu Y, Peng CK, Novak V (2008) Multimodal pressure flow analysis: application of Hilbert–Huang transform in cerebral blood flow regulation. EURASIP J Adv Signal Process 2008:785243
18. Ponomarenko VI, Prokhorov MD, Bespyatov AB, Bodrov MB, Gridnev VI (2005) Deriving main rhythms of the human cardiovascular system from the heartbeat time series and detecting their synchronization. Chaos Solitons Fractals 23:1429–1438
19. Rajendra Acharya U, Paul Joseph K, Kannathal N, Lim CM, Suri JS (2006) Heart rate variability: a review. Med Biol Eng Comput 44:1031–1051
20. Rilling G, Flandrin P, Gonçalvès P (2003) On empirical mode decomposition and its algorithm. In: Proceedings of the 6th IEEE/EURASIP workshop on nonlinear signal and image processing (NSIP'03), Grado, Italy, June 8–11
21. Task force of the European society of cardiology and the north american society of pacing and electrophysiology (1996) Heart rate variability: standards of measurement, physiological interpretation and clinical use. Circulation 93:1043–1065
22. von Ballmoos MW, Takala J, Roeck M, Porta F, Tueller D, Ganter CC, Schröder R, Bracht H, Baenziger B, Jakob SM (2010) Pulse-pressure variation and hemodynamic response in patients with elevated pulmonary artery pressure: a clinical study. Crit Care 14:P111
23. MC Wu, CK Hu (2006) Empirical mode decomposition and synchrogram approach to cardiorespiratory synchronization. Phys Rev E Stat Nonlinear Soft Matter Phys 73:051917
24. Wu MC, Huang NE (2009) Biomedical data processing using HHT: a review. Adv Biosignal Process Amine NAIT-ALI Ed. Chapter 19 Springer 335–352
25. Wu Z, Huang NE (2009) Ensemble empirical mode decomposition: a noise assisted data analysis method. Adv Adapt Data Anal 1:1–42
26. Wu HT, Lee CH, Liu AB, Chung WS, Tang CJ, Sun CK, Yip HK (2011) Arterial stiffness using radial arterial waveforms measured at the wrist as an indicator of diabetic control in the elderly. IEEE Trans Biomed Eng 58:243–252
27. Yang Z, Yang L, Qing C (2010) An oblique-extrema-based approach for empirical mode decomposition. Digit Signal Proc 20:699–714
28. Yeh JR, Sun WZ, Shieh JS, Huang NE (2010) Investigating fractal property and respiratory modulation of human heartbeat time series using empirical mode decomposition. Med Eng Phys 32:490–496
29. Yeh JR, Shieh JS, Huang NE (2010) Complementary ensemble empirical mode decomposition: a novel noise enhanced data analysis method. Adv Adapt Data Anal 2:243–252